

# Synthesis of Nanocrystalline Tetragonal Zirconia by a Polymeric Organometallic Method

Antonio L. Quinelato,<sup>1\*</sup> Elson Longo,<sup>2</sup> Edson R. Leite<sup>2</sup> and José A. Varela<sup>3</sup>

<sup>1</sup>CNEN/COLAB, Poços de Caldas, MG, 37701-970 Brazil

<sup>2</sup>Departamento de Química, UFSCar, São Carlos, SP, 13565-905 Brazil

<sup>3</sup>Instituto de Química, UNESP, Araraquara, SP, 14800-900 Brazil

A polymeric precursor method based on the Pechini process was successfully used to synthesize zirconia–12 mol% ceria ceramic powders. The influence of the main process variables (citric acid–ethylene glycol ratio, citric acid–total oxides ratio and calcination temperature) on phase formation and powder morphology (surface area and crystallite size) were investigated. The thermal decomposition behavior of the precursor is presented. X-ray diffraction (XRD) patterns of powders revealed a crystalline tetragonal zirconia single-phase, with crystallite diameter ranging from 6 to 15 nm. The BET surface areas were relatively high, reaching 95 m<sup>2</sup> g<sup>-1</sup>. Nitrogen adsorption/desorption on the powders suggested that nonaggregated powders could be attained, depending on the synthesis conditions. Copyright © 1999 John Wiley & Sons, Ltd.

**Keywords:** Pechini process; zirconia; ceramic; x-ray diffraction

Received 4 April 1998; accepted 1 October 1998

## INTRODUCTION

Zirconia is an important ceramic material widely employed in differing fields such as refractories, cutting tools, oxygen sensors and electrolytes.<sup>1</sup> Pure zirconia undergoes a reversible diffusionless martensitic monoclinic–tetragonal phase transformation at about 1200 °C.<sup>1,2</sup> This transformation is

associated with a large volume change, so that severe cracking often appears if ceramics are cycled through the transition temperature, which renders the material useless for structural applications. Thus, during normal processing the high-temperature tetragonal phase must be stabilized at room temperature to avoid this problem. The stabilization is achieved by making solid solutions with several oxides.<sup>1</sup> Ceria-doped zirconia can result in a single-phase tetragonal structure, which possesses excellent mechanical properties. The tetragonal phase stability is dependent on the solubility limit described in the temperature–composition equilibrium phase diagram.<sup>3</sup> The alloy containing 12 mol% CeO<sub>2</sub> was found to be more attractive for its high fracture toughness.<sup>4</sup> The crystallite size effect on the stabilization of tetragonal zirconia has been observed.<sup>5,6</sup> Garvie<sup>7</sup> explained this effect by taking into account that the surface energy of the tetragonal phase is less than that of the monoclinic structure.<sup>8</sup> Thus, the tetragonal form is more stable in small crystallites and, if a critical crystallite size is exceeded, the tetragonal particles are transformed to the monoclinic phase.

Recently, wet-chemical methods have been employed with the aim of producing ceramic powders with high purity, compositional homogeneity, precise stoichiometry and fine particles. Among different methods, the application of polymeric precursors based on the process originally outlined by Pechini<sup>9</sup> has been used in the preparation of a wide variety of ceramic oxides, such as titanates,<sup>10,11</sup> perovskites,<sup>12–15</sup> aluminates,<sup>16</sup> spinels<sup>17</sup> and superconductors.<sup>18,19</sup>

In the Pechini process described in the original patent,<sup>9</sup> an  $\alpha$ -hydroxycarboxylic acid, preferably citric acid, is used to chelate various cations by forming a polybasic acid. In the presence of a polyhydroxy alcohol, normally ethylene glycol, these chelates react with the alcohol to form ester and water by-products. When the mixture is heated,

\* Correspondence to: Antonio L. Quinelato, CNEN/COLAB, Poços de Caldas, MG, 37701-970 Brazil.

Contract/grant sponsor: FINEP.

Contract/grant sponsor: CNPQ.

Contract/grant sponsor: CNEN/COLAB.

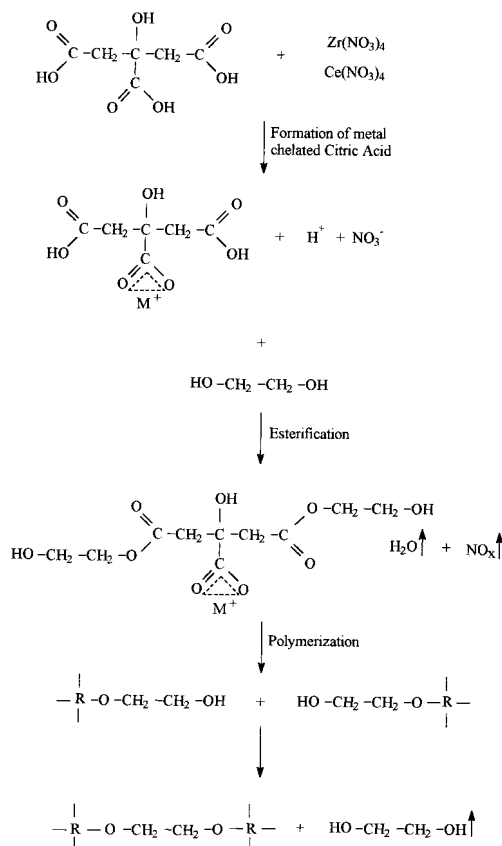


**Figure 1** The chemical reactions involved in the polymeric precursor synthesis.

polyesterification occurs in the liquid solution and results in a homogeneous sol, in which metal ions are uniformly distributed throughout the organic polymeric matrix. When excess solvents are removed, an intermediate resin is formed. The metal ions remain homogeneously distributed in the polymeric chain, because of the high viscosity of the resin and the strong coordination interactions associated with the complex. The basic chemical reactions involved in the Pechini method are presented in a schematic illustration (Fig.1). The resin is charred and calcined to remove all organic substances and to yield oxide powders.

This method was also applied to zirconia–ceria<sup>20</sup> and zirconia–yttria<sup>21</sup> powder synthesis. The method is effective in preparing zirconia with a tetragonal structure, as demonstrated by these studies. However, few systematic investigations have been done with the aim of evaluating the influence of synthesis variables on the powder properties of zirconia-

based ceramics, using polymeric precursor methods.

A polymeric method based on the Pechini process has been used in the present study to synthesize  $\text{ZrO}_2$ –12 mol%  $\text{CeO}_2$  powders. The objective was to evaluate the influence of process variables such as the citric acid/ethylene glycol ratio, the citric acid/total oxides ratio and the calcination temperature on the stabilization of tetragonal zirconia at room temperature and the powder morphology regarding surface area and crystallite size. Thermal decomposition of the polymeric precursors was also considered.

## EXPERIMENTAL PROCEDURE

### Preparation of zirconium and cerium solutions

A 91.5 g portion of zirconium(IV) oxychloride,  $\text{ZrOCl}_2 \cdot 8\text{H}_2\text{O}$  (purity >99.5%; Merck, Darmstadt, Germany) was first dissolved in 2000 ml distilled water. Zirconium hydroxide was precipitated from this solution by adding ammonium hydroxide to pH 8.0. The solution thus obtained was then filtered, the liquid phase was discarded and the zirconium hydroxide was washed with distilled water until chloride ions in the liquid phase had been eliminated completely. The zirconium hydroxide was then dissolved with 150 ml nitric acid (65%, w/w). Distilled water was added to obtain 1000 ml of zirconium nitrate solution containing  $35 \text{ g l}^{-1}$   $\text{ZrO}_2$ .

Cerium hydroxide (purity >99%; Nuclemon, São Paulo, Brazil) (8.5 g) was dissolved in 200 ml nitric acid (65%, w/w) at 80 °C, then distilled water was added to obtain 350 ml of cerium nitrate solution containing  $20 \text{ g l}^{-1}$   $\text{CeO}_2$ .

### Synthesis

Zirconium nitrate (30 ml) and cerium nitrate (10 ml) solutions were mixed in a beaker, taking into account the stoichiometry  $\text{ZrO}_2$ –12 mol%  $\text{CeO}_2$  in the final ceramic powder. With stirring, the mixture was heated at about 100 °C. Citric acid (CA) was added at a CA/total oxides molar ratio (CA/TO) of 4:1. Total oxides denote the sum of  $\text{ZrO}_2$  plus  $\text{CeO}_2$  in the final ceramic powder. After 15 min ethylene glycol (EG) was added to solution at various CA/EG molar ratios, i.e. 1:10, 1:5, 1:2, 1:1, 1.5:1 and 2:1. The solution was then heated to

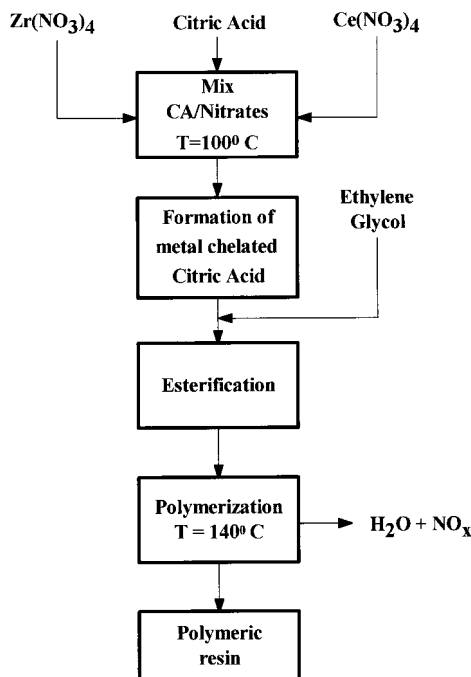


**Figure 2** Synthesis of the polymeric precursor for production of  $\text{ZrO}_2$ –12 mol%  $\text{CeO}_2$  powders.

140 °C, to promote the polyesterification reaction. After 40 min, when nitrous oxides and water were eliminated, a white resin was obtained. These procedures are outlined in the flow chart (Fig. 2). Two feasible structures of the polymer are presented in a schematic illustration (Fig. 3). The polymeric resin was charred at 250 °C to remove organic matter. Char flakes were obtained, which were dry ball-milled to obtain particle sizes below 150  $\mu\text{m}$ . The black powder thus produced was calcined for 2 h in a crucible at various temperatures, i.e. 400, 500, 600, 700 and 800 °C, to obtain the  $\text{ZrO}_2$ – $\text{CeO}_2$  ceramic powder.

Further synthesis assays were performed using CA/TO molar ratios of 2:1 and 6:1, to evaluate the influence of this process variable on the existing phase and powder morphology (surface area and crystallite size).

### Characterization of precursor and ceramic powders

Thermal decomposition of the polymeric precursor was investigated by thermogravimetry–differential thermal analysis (Netsch, model STA 409), in atmospheric air, where the heating rate was 10 °C

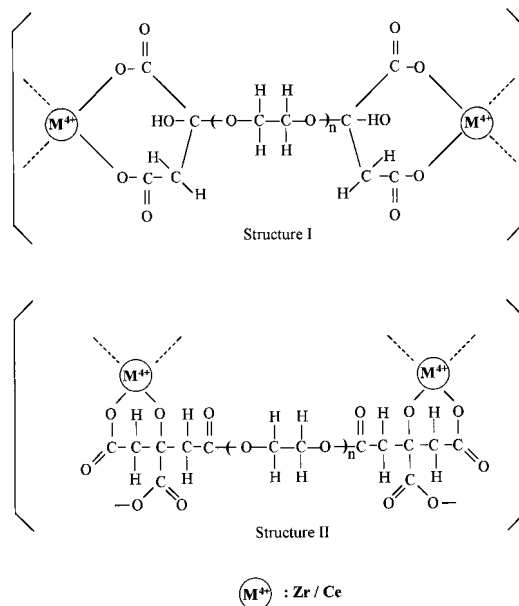


**Figure 3** The polymer structures.

$\text{min}^{-1}$  and the temperature ranged from 20 to 800 °C. The existing phases in the ceramic powders were investigated by X-ray diffraction (XRD) (Siemens diffractometer, model D-5000, with  $\text{CuK}\alpha$  radiation and a graphite monochromator). Powder crystallite size was determined using the X-ray line broadening method, by the Scherrer equation.<sup>22,23</sup> Nitrogen adsorption/desorption on the powder surface at 77 K (Micromeritics, ASAP 2000) was used to verify the occurrence of hysteresis and to measure the specific surface area by applying the BET method.<sup>24</sup>

## RESULTS AND DISCUSSION

The thermal decomposition of polymeric precursors synthesized at CA/EG = 2:1 (Fig. 4) shows weight losses in two distinct regions, namely, 100–400 °C and 400–600 °C. The first region, below 400 °C, with higher weight loss, was associated with charring of the polymer, i.e. conversion of the organic component of the precursor of free carbon. The second region showed a sharp exothermic peak resulting from char burnout. For other CA/EG ratios the thermal decomposition behavior was similar. The total weight losses (Table 1) were

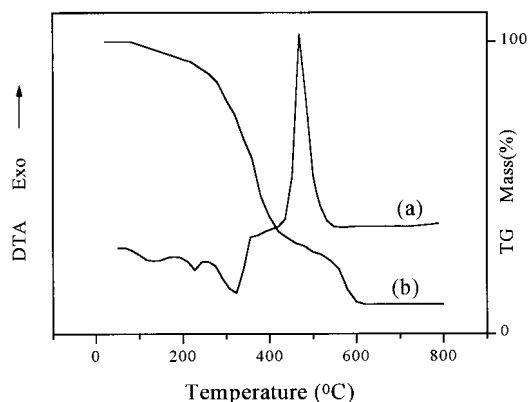


**Figure 4** (a) Differential thermal analysis traces of polymeric precursors synthesized at CA/EG = 2:1. (b) Typical thermogravimetric analysis curve of polymeric precursor. CA/TO = 4:1.

proportional to the amount of organic component present.

The XRD patterns for the powders synthesized at CA/EG = 2:1 and CA/TO = 4:1, calcined at different temperatures (Fig. 5), show the presence of amorphous material at 400 and 500 °C, indicating that at these temperatures there is still organic material present. With increasing calcination temperature (above 600 °C) a well-resolved XRD patterns are observed, showing total crystallization in a tetragonal single-phase. This indicates that all organic material was burned at temperatures above 600 °C, compatible with the total weight loss results (Fig. 4). A similar behavior was obtained for other CA/EG ratios.

The XRD patterns for the powders synthesized at different CA/EG ratios and calcined at 600 °C (Fig. 6) show a crystalline tetragonal zirconia, single-phase for all CA/EG ratios investigated. This behavior was also observed for samples calcined at 700 and 800 °C. The tetragonal single-phase was also attained for powders synthesized at CA/TO = 2:1 and 6:1. Thus, tetragonal zirconia–ceria powders were synthesized by use of polymeric precursors.

Both calcination temperature and CA/EG ratio (Fig. 7) affected the crystallite size. Increase in calcination temperature provided exponential growth of crystallites, denoting a rapid coarsening of particles when the powders are heated. Increase in amount of ethylene glycol favored decrease in crystallite size. This increase in ethylene glycol

**Table 1** Total weight loss during thermal decomposition of the polymeric precursors

CA/EG ratio (mol mol <sup>-1</sup> )	Total weight loss (%)
1:10	96.8
1:5	94.8
1:2	91.2
1:1	91.0
1.5:1	89.9
2:1	88.9

promotes an increase in the polymeric chain length (higher *n* value, in the structures in Fig. 3), increasing the distance between chelated cations. This suggests that the crystallization of primary particles during calcination of the charred resin occurs more independently. That is, the interactions become weaker among particles with an increase in the amount of ethylene glycol, so smaller particles are obtained. The method used provided nanosized ZrO<sub>2</sub>–12 mol% CeO<sub>2</sub> powders. The mean crystallite diameter attained ranged from 6 to 15 nm.

Consequently, a decrease in calcination temperature and an increase in the amount of ethylene glycol increase the specific surface areas of the powders (Fig. 8), due to diminution of particle sizes. As shown in Fig. 8 the surface area increases linearly with decreasing temperature. However, this increase in proportion to the lowering in temperature became slightly smaller with the diminution in amount of ethylene glycol, probably due to an increase in particle aggregation. With decreasing amount of ethylene glycol, the distance between the crystallized primary particles during calcination becomes shorter, making possible a more intense

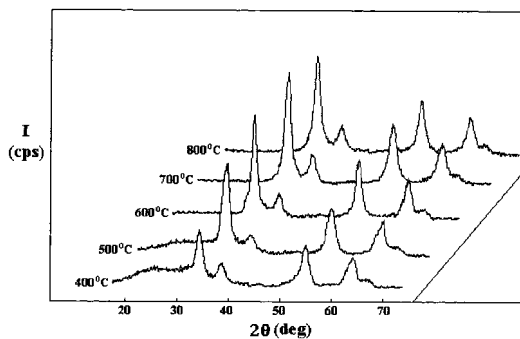


**Figure 5** X-ray diffraction patterns of ZrO<sub>2</sub>–12 mol% CeO<sub>2</sub> powders synthesized at CA/EG = 2:1, CA/TO = 4:1, and calcined at different temperatures.

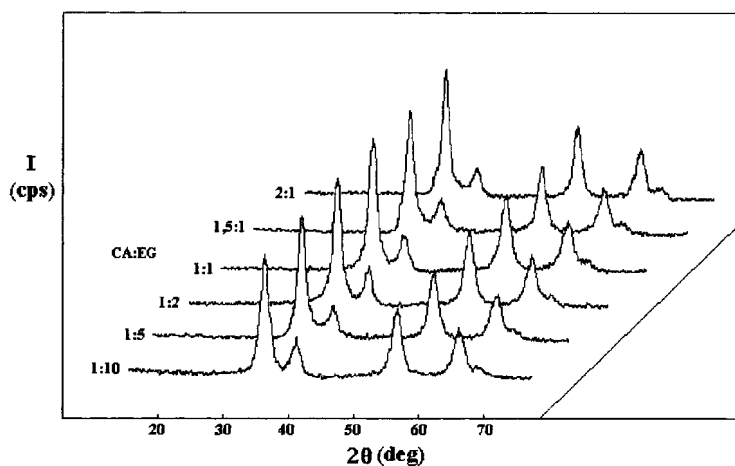


**Figure 6** X-ray diffraction patterns of  $\text{ZrO}_2$ -12 mol%  $\text{CeO}_2$  powders synthesized at  $\text{CA}/\text{TO} = 4:1$ , and different  $\text{CA}/\text{EG}$  ratios. Calcination temperature = 600 °C.

aggregation by solid-state diffusion, and thus reducing the surface areas.

As observed (Table 2), the  $\text{CA}/\text{TO}$  ratio did not influence significantly the crystallite size of the powders synthesized at  $\text{CA}/\text{EG} = 1:5$ , but it affected the surface area. Higher areas were obtained at  $\text{CA}/\text{TO} = 4:1$ , indicating less or no aggregation.

The nitrogen adsorption/desorption isotherms for the powder synthesized at  $\text{CA}/\text{EG} = 1:5$  and  $\text{CA}/\text{TO} = 4:1$  (Fig. 9a) were coincident, i.e., a hysteresis was not observed, indicating that capillary con-

densation in mesopore structures did not occur.<sup>24</sup> This suggests the absence, or presence of only small quantities, of particle aggregates. The behavior of powders synthesized using the other  $\text{CA}/\text{EG}$  ratios, and the same  $\text{CA}/\text{TO}$  ratio (4:1) was similar. However, a hysteresis was observed for the powders synthesized at  $\text{CA}/\text{TO} = 2:1$  and 6:1, using  $\text{CA}/\text{EG} = 1:5$  (Fig. 9b and 9c, respectively), denoting the presence of greater quantities of particle aggregates, which probably induced the lower

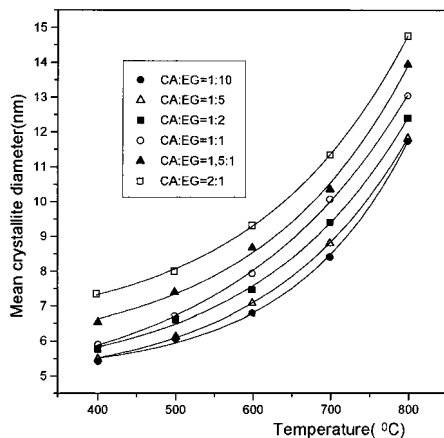


**Figure 7** Crystallite diameter of  $\text{ZrO}_2$ -12 mol%  $\text{CeO}_2$  powders as a function of calcination temperature.  $\text{CA}/\text{TO} = 4:1$ .

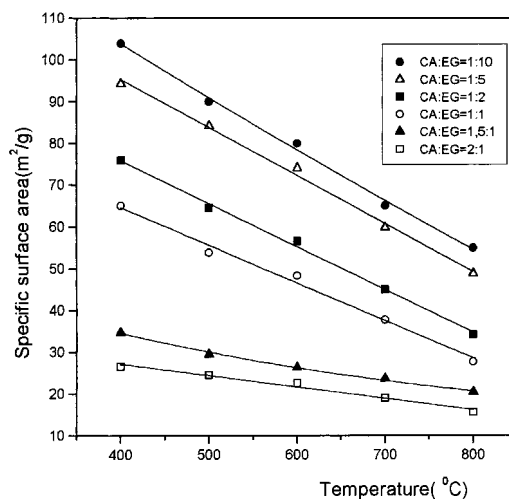


**Figure 8** Surface area of  $\text{ZrO}_2$ -12 mol%  $\text{CeO}_2$  powders as a function of calcination temperature.  $\text{CA}/\text{TO} = 4:1$ .

**Table 2** Mean crystallite diameter ( $D$ ) and BET surface area (SA) for powders synthesized at CA/EG = 1:5, and different CA/TO molar ratios (calcination temperature = 600 °C.)

CA/TO (mol mol <sup>-1</sup> )	$D$ (nm)	SA (m <sup>2</sup> g <sup>-1</sup> )
2:1	7.13	42.9
4:1	7.10	74.1
6:1	7.02	60.7

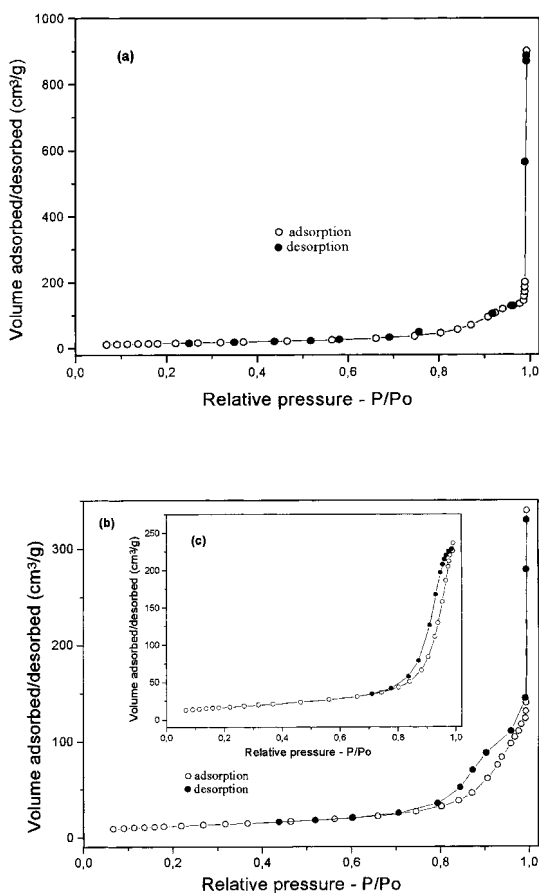


**Figure 9** Nitrogen adsorption/desorption isotherms for the  $\text{ZrO}_2$ -12 mol%  $\text{CeO}_2$  powders synthesized at CA/EG = 1:5 and calcined at 600 °C. (a) CA/TO = 4:1; (b) CA/TO = 2:1; (c) CA/TO = 6:1.

surface areas of these powders compared with the nonaggregated, high surface area, powder synthesized at CA/TO = 4:1 (Table 2). These results show that the CA/TO ratio affected the aggregate formation. The physical morphology of the final

oxide powder made by a Pechini-type method is influenced by the morphologies of their charred resin intermediates.<sup>15,25,26</sup> At CA/TO ratios of 2:1 and 6:1, rigid charred resins were observed, while at a CA/TO ratio of 4:1 a soft material was attained. Thus, the rigidity suggests aggregation, i.e. non-aggregated powder cannot be attained when a rigid charred resin intermediate is produced.

## CONCLUSIONS

Nanocrystalline, high specific surface area (reaching 95 m<sup>2</sup> g<sup>-1</sup>), tetragonal, single-phase  $\text{ZrO}_2$ -12 mol%  $\text{CeO}_2$  was synthesized chemically, using a polymeric precursor method. Nonaggregated powders can be attained, depending on the synthesis conditions used. The studies revealed that the process variables citric acid/ethylene glycol ratio, and calcination temperature affected significantly the powder morphology regarding surface area and crystallite size. The citric acid/total oxides ratio affected the particle aggregate formation, and nonaggregated powder was obtained for a 4:1 ratio.

**Acknowledgements** The authors acknowledge FINEP, CNPQ and CNEN/COLAB for financial support of this work.

## REFERENCES

1. R. Stevens, in: *Magnesium Elektron Publication*, No. 113 Zirconia and Zirconia Ceramics, New Jersey (1986), pp. 1-52.
2. E. C. Subbarao, in: *Science and Technology of Zirconia*, Heuer, A. H. and Hobbs, L. W. (eds), Vol. 3 of *Advances In Ceramics*, The American Ceramic Society, Columbus, OH, 1981.
3. M. Yashima, H. Takashima, M. Kakihana and M. Yoshimura, *J. Am. Ceram. Soc.* **77**, 1869 (1994).
4. K. Tsukuma and M. Shimada, *J. Mater. Sci.* **20**, 1178 (1985).
5. R. H. J. Hannink, K. A. Johnston, R. T. Pascoe and R. C. Garvie, pp. 116-36 in: *Science and Technology of Zirconia*, Heuer, A. H. and Hobbs, L. W. (eds), Vol. 3 of *Advances In Ceramics*, The American Ceramic Society, Columbus, OH, 1981.
6. V. S. Nagarajan and K. J. Rao, *J. Mater. Res.* **6**, 2688 (1991).
7. R. C. Garvie, *J. Phys. Chem.* **82**, 218 (1978).
8. H. F. Holmes, E. L. Fuller Jr and R. B. Gammage, *J. Phys. Chem.* **76**, 1497 (1972).
9. M. P. Pechini, US Patent 3 330 697 (11 July 1967).

10. S. Kumar, G. L. Messing and W. B. White, *J. Am. Ceram. Soc.* **76** 617 (1995).
11. M. Cerqueira, R. S. Nasar, E. Longo, E. R. Leite and J. A. Varela, *Mater. Lett.* **22**, 181 (1995).
12. G. K. Chuah, S. Jaenicke, K. S. Chan, S. T. Khor and J. O. Hill, *J. Thermal Anal.* **40**, 1157 (1993).
13. M. Liu and D. Wang, *J. Mater. Res.* **10**, 3210 (1995).
14. M. V. -Regí, C. V. Rangel, J. Ramírez and J. M. G. -Calbet, *Sol. State Ion.* **63–65**, 60 (1993).
15. L.-W. Tai and P. Lessing, *J. Mater. Res.* **7**, 511 (1992).
16. M. A. Gülgün, O. O. Poppola and W. M. Kriven, *J. Am. Ceram. Soc.* **77** 531 (1994).
17. W. Liu, G. C. Farrington, F. Chaput and B. Dunn, *J. Electrochem. Soc.* **143**, 879 (1996).
18. Y. K. Tao and P. H. Hor, *Mater. Chem. Phys.* **35**, 92 (1993).
19. C. Chiang, Y. T. Huang and C. Y. Shei, *Chin. J. Mater. Sci.* **25**, 50 (1993).
20. M. Yashima, K. Ohtake, M. Kakihana and M. Yoshimura, *J. Am. Ceram. Soc.* **77**, 2773 (1994).
21. H. Salze, P. Odier and B. Cales, *J. Non-Cryst. Sol.* **82**, 314 (1986).
22. H. Klug and L. Alexander, in: *X-ray Diffraction Procedures*, John Wiley and Sons New York, 1954, pp.491–538.
23. E. W. Nuffield, in: *X-ray Diffraction Methods*, John Wiley and Sons, New York, 1986, pp. 147–148.
24. K. S. Sing, *Pure Appl. Chem.*, **54**, 2201 (1982).
25. P. A. Lessing, *Ceram. Bull.* **68**, 1002 (1989).
26. L.-W. Tai and P. Lessing, *J. Mater. Res.* **7**, 502 (1992).